Full Length Article

Multicomponent patterned ultrathin carbon nanomembranes by laser ablation

Natalie Frese [a], Julian Scherr [b], André Beyer [a], Andreas Terfort [b], Armin Gölzhäuser [a], Norbert Hampp [c], Daniel Rhinow [d],*

[a] *University of Bielefeld, Faculty of Physics, Universitätsstr. 25, D-33615, Bielefeld, Germany*
[b] *Goethe-University Frankfurt, Department of Chemistry, Max-von-Laue-Str. 9, D-60438, Frankfurt, Germany*
[c] *Philipps-University Marburg, Department of Chemistry, Hans-Meerwein-Str. 4, D-35032, Marburg, Germany*
[d] *Max Planck Institute of Biophysics, Department of Structural Biology, Max-von-Laue-Str. 3, D-60438, Frankfurt, Germany*

ABSTRACT

Carbon nanomembranes (CNMs) are a class of two-dimensional materials, which are obtained by electron beam-induced crosslinking of aromatic self-assembled monolayers (SAMs) on solid substrates. CNMs made from a single type of precursor molecule are uniform with homogeneous chemical and physical properties. We have developed a method for the fabrication of internally patterned CNMs resembling a key feature of biological membranes. Direct laser patterning is used to obtain multicomponent patterned SAMs on gold, which are subsequently crosslinked by electron irradiation. We demonstrate that the structure of internally patterned CNMs is preserved upon transfer to different substrates. The method enables rapid fabrication of patterned 2D materials with local variations in chemical and physical properties on the micrometer to centimeter scale.

© 2017 Elsevier B.V. All rights reserved.

1. Introduction

A technologically interesting feature of biological membranes is the formation of complex patterns by two-dimensional self-assembly of biomolecular building blocks in a 5 nm thin lipid matrix [1]. Self-assembled monolayers (SAMs) of thiols on gold have been studied extensively as model systems for self-assembly and pattern formation in two dimensions [2,3]. A variety of techniques has been used to pattern SAMs including UV lithography [4,5], microcontact printing [6], dip pen lithography [7], electron beam lithography [8,9], and direct laser patterning [10–15]. Direct laser patterning (DLP) of SAMs enables rapid fabrication of multicomponent surface structures with lateral dimensions in the micrometer to centimeter range [13], which is particularly useful for the fabrication of protein-surface [16] and cell-surface interfaces [17]. However, patterned thiol SAMs are not stable in the absence of the gold support, which precludes their transfer as a continuous membrane to another substrate.

It has been shown that SAMs of aromatic thiols can be crosslinked by irradiation with low-energy electrons [18]. Upon removal of the gold substrate, 1 nm thin free-standing carbon nanomembranes (CNMs) were obtained [19–21]. Depending on the aromatic precursor molecule, thickness and mechanical properties of CNMs can be tuned [22]. Owing to their low thickness, CNMs have been successfully applied as support films for transmission electron microscopy of biological specimens [23,24]. Furthermore, chemically patterned CNMs have been used as templates for the fabrication of nanostructures such as polymer carpets [25] or bio-hybrid assemblies [26].

CNMs made from a single precursor molecule are in principle uniform. Selective electron beam-induced crosslinking of aromatic SAMs, followed by exchange of thiols in the non-exposed areas and subsequent crosslinking of the heterogeneous SAM has been applied to fabricate chemically patterned CNMs [27]. A disadvantage of this method is the fact that crosslinked areas cannot be patterned multiple times. In this work, we used DLP to fabricate internally patterned CNMs and transferred them to different substrates. DLP enables rapid fabrication of chemically patterned aromatic SAMs, which are subsequently crosslinked to form internally patterned ultrathin CNMs with locally varying chemical and physical properties. Internally patterned CNMs were analyzed by X-
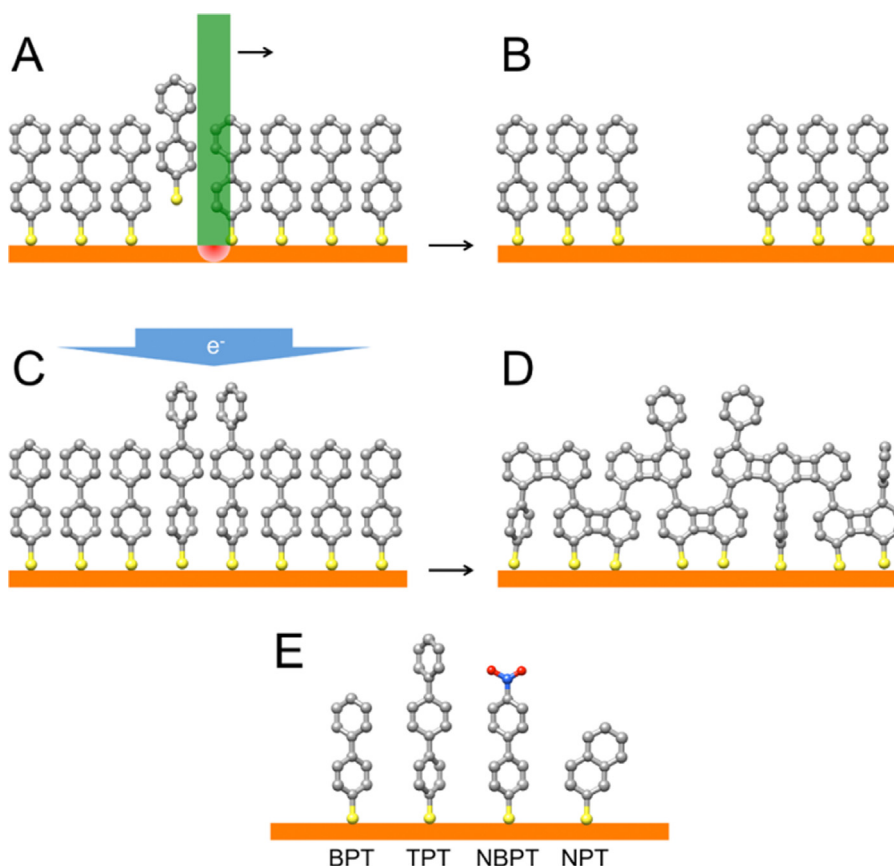
Fig. 1. Fabrication of internally patterned CNMs by direct laser patterning. (A) A SAM of aromatic thiols is formed on a gold surface. The SAM consists of BPT molecules. A focused laser beam ($\lambda = 532$ nm) is used to impart thermal energy to a confined area on the gold substrate causing desorption of aromatic thiols (B). (C) The gaps are filled with a second thiol, in this case TPT. Irradiation with low-energy electrons causes crosslinking of the aromatic thiols. (D) Internally patterned CNM. (E) Aromatic thiols used for the fabrication of patterned CNMs. BPT: 1′-Biphenyl-4-thiol; TPT: [1″,4′,1′,1]-terphenyl-4-thiol; NBPT: 4′-nitro-1,1′-biphenyl-4-thiol; NPT: naphthalene-2-thiol. Owing to the generation of hydrogen radicals during crosslinking, the nitro groups of NBPT are converted to amino groups (4′-amino-1,1′-biphenyl-4-thiol: ABPT) [29].

ray photoelectron microscopy (XPS), scanning electron microscopy (SEM) and helium ion microscopy (HIM).

2. Materials and methods

2.1. Chemicals

1,1′-Biphenyl-4-thiol (BPT), [1″,4′,1′,1]-terphenyl-4-thiol (TPT), and naphthalene-2-thiol (NPT) were purchased from Sigma-Aldrich (St. Louis, USA), 4′-nitro-1,1′-biphenyl-4-thiol (NBPT) was purchased from Taros Chemicals. Gold on silicon with titanium adhesion layer was purchased from Georg Albert PVD (Silz, Germany). Gold substrates suitable for subsequent transfer of patterned CNMs were made by depositing 200 nm of gold onto polished ⟨100⟩ silicon wafers. SAMs were formed by immersion in 10 mM solutions of aromatic thiols in organic solvents at room temperature. We used acetone (BPT, TPT, NPT), heptane (BPT), toluene (BPT, TPT), and dimethylformamide (NBPT) as solvents.

2.2. Direct laser patterning

DLP of aromatic thiols on gold was accomplished with a frequency-doubled Nd:YVO$_4$ diode pumped solid state laser (Explorer XP 532-5, Newport, USA) emitting 6 ns pulses (FWHM) with a 50 kHz repetition rate at a wavelength of $\lambda = 532$ nm. Photons of this wavelength are absorbed by the gold surface only. The laser beam was focused to a spot diameter of 15 μm. In previous work, the optimum energy deposited to the sample was deter-

mined to 111 MW/cm^2 [11]. The energy deposited to the sample was adjusted with a polarizing beam splitter coupled to a polarizer. To optimize the patterning result, SAMs were patterned with decreasing laser power. After laser irradiation, patterned SAMs were immersed in a solution of the second thiol at room temperature.

2.3. Transfer of patterned CNMs

Damage-free transfer of CNMs was accomplished as described previously [20]. For the transfer of the patterned CNM, the film was protected with a double-layer of poly(methylmethacrylate) (PMMA) by spin-coating. Then the gold was exfoliated by angular dipping of the silicon wafer into water. The floating film on water was transferred to different solutions using a piece of silicon wafer. The gold was etched by placing the thin gold film on an aqueous iodine solution (10 wt% potassium iodide, 2.5 wt% iodine in water). Afterwards the PMMA-protected patterned CNM was placed on an aqueous potassium iodide solution (10 wt% potassium iodide in water). Finally, the film was transferred to a substrate (silicon or gold), the PMMA was removed by immersion in acetone for 2 h, and the substrate was dried in a stream of nitrogen.

2.4. Scanning electron microscopy (SEM)

Samples were analyzed in a Zeiss Auriga at an acceleration voltage of 5 kV using the in-lens detector for secondary electrons.
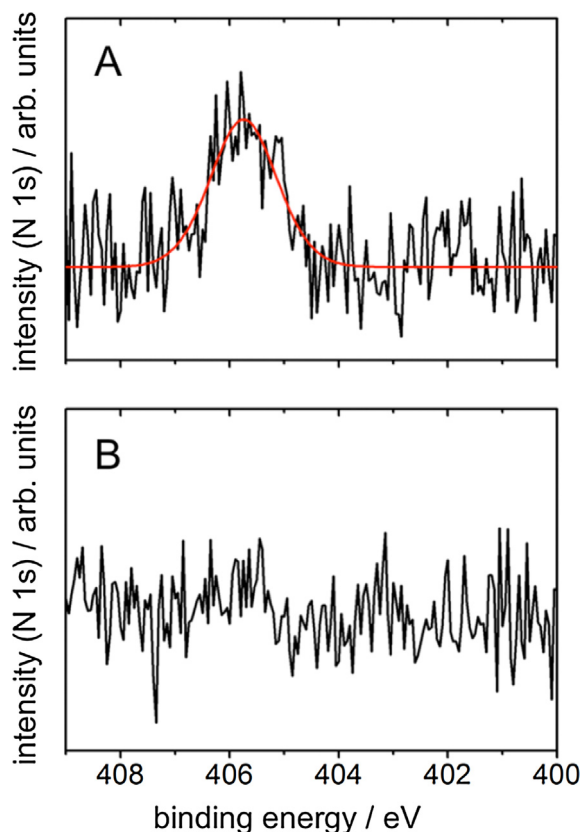
Fig. 2. Incorporation of NBPT into a BPT SAM with and without DLP. (A) XP spectrum obtained from a BPT SAM after laser irradiation and subsequent immersion in a solution containing NBPT for 72 h. The spectrum reveals the N 1 s peak at 405.7 eV indicating the incorporation of NBPT. (B) XP spectrum of a BPT sample, which was immersed in a solution containing NBPT for 72 h. The N 1 s peak is absent.

2.5. Helium ion microscopy (HIM)

Samples were imaged in a Zeiss Orion Plus at acceleration voltages between 30 and 36 kV and currents between 0.4–4 pA. An electron floodgun was used to mitigate electrostatic charging while secondary electrons were detected with an Everhart-Thornley detector.

2.6. X-ray photoelectron spectroscopy (XPS)

Samples were analyzed in an Omicron Multiprobe UHV system using monochromatic Al Kα irradiation, a Sphera electron analyzer with a resolution of 0.9 eV and an emission angle of 20°.

3. Results and discussion

Fig. 1 illustrates the use of DLP to fabricate internally patterned CNMs consisting of crosslinked aromatic SAMs on a gold surface. This approach enabled us to fabricate patterned CNMs from a variety of aromatic precursor molecules (Fig. 1E).

To confirm that laser irradiation leads to spatially selective desorption of aromatic thiols by photothermal cleavage of the gold-sulfur bond (Fig. 1A and B), we analyzed the incorporation of NBPT into a BPT SAM with and without prior laser irradiation.

Fig. 2A shows XP spectra of a BPT SAM, which was irradiated with a focused laser beam (λ = 532 nm) and subsequently immersed in a solution containing NBPT. The XP spectrum reveals the N 1 s signal at a binding energy of 405.7 eV, indicating the incorporation of NBPT molecules into gaps formed by photothermal desorption of BPT molecules. Our experiments are in accordance with previous

results obtained with DLP of NBPT SAMs [28]. Without prior laser irradiation, immersion of a BPT SAM on gold in a solution containing NBPT does not lead to incorporation of NBPT as confirmed by XPS (Fig. 2B). This demonstrates that self-exchange of aromatic thiols at room temperature is negligible at the time scale of a few days.

It is of critical importance that the structure of patterned SAMs is preserved after electron beam-induced crosslinking. We analyzed a patterned BPT SAM, consisting of TPT lines written into a BPT SAM, by HIM before (Fig. 3A) and after (Fig. 3B) crosslinking with electrons. Fig. 3C shows an SEM image of the same sample after crosslinking. Our experiments reveal that structure and chemical contrast of patterned aromatic thiol SAMs are preserved after crosslinking by electron irradiation.

Our experiments reveal that structure and chemical contrast of patterned aromatic thiol SAMs are preserved after crosslinking by electron irradiation. Furthermore, our analysis enables a direct comparison of HIM and SEM as tools for imaging patterned SAMs. SEM is suitable for the analysis of patterned SAMs as thiols produce chemical contrast in the secondary electron image in dependence of chain length, terminal groups, and acceleration voltage [30–33]. Recently, HIM has been used to analyze monolayers on solid substrates [34,35]. Interestingly, the same pattern appears with different contrast in HIM and SEM SE images. The TPT lines appear with a dark center and a bright rim in the HIM image (Fig. 3B), whereas in the SEM image TPT lines appear uniformly darker than the BPT matrix. This could be explained by the fact that in the SEM most secondary electrons (SE) are generated in the gold substrate and their contrast is determined by a stronger attenuation in TPT, as compared to BPT. Conversely, contrast in the HIM images is largely determined by SE generated in the organic film and is more influenced by the film's thickness and topography. On the other hand, it may also be that local heating of the gold substrate during DLP causes subtle rearrangements in the gold, which cause changes in SE contrast in HIM images only, owing to the high sensitivity of HIM towards surface chemistry. More work on charge-particle interaction in molecular films is needed to understand the subtle differences in the contrasts of HIM and SEM images.

The formation of mechanically stable membranes was confirmed by successful transfer of internally patterned CNMs to other substrates. Fig. 4A shows wetting patterns on a patterned CNM after transfer to a gold substrate, observed by light microscopy upon exposing the sample to humid air. Although quantitative description of wetting patterns is difficult, wetting is a fast method to visualize chemical patterns by light microscopy. Areas containing ABPT and BPT can be clearly distinguished in HIM (Fig. 4B) and SEM (Fig. 4C) SE images of the same sample.

It has been shown earlier that DLP can be used to fabricate patterned SAMs of arbitrary complexity [13]. We applied DLP to fabricate internally patterned CNMs consisting of three different types of aromatic molecules (Fig. 4D). Fig. 4D shows a SEM image of a transferred patterned CNM consisting of patterns of BPT, TPT, and NPT, which demonstrates that DLP enables the fabrication of multicomponent patterned CNM. In difference to SE images of crosslinked patterned SAMs, acquired before transfer to other substrates (Fig. 3B and C), transferred membranes produce identical contrast in HIM and SEM images (Fig. 4B and C). The mechanisms behind contrast generation in HIM SE images of monolayers on solid substrates require further elucidation.

4. Conclusions

We have demonstrated that DLP is a versatile tool for the fabrication of internally patterned CNMs. Like biological membranes, patterned CNMs consist of distinct chemical domains, which cause
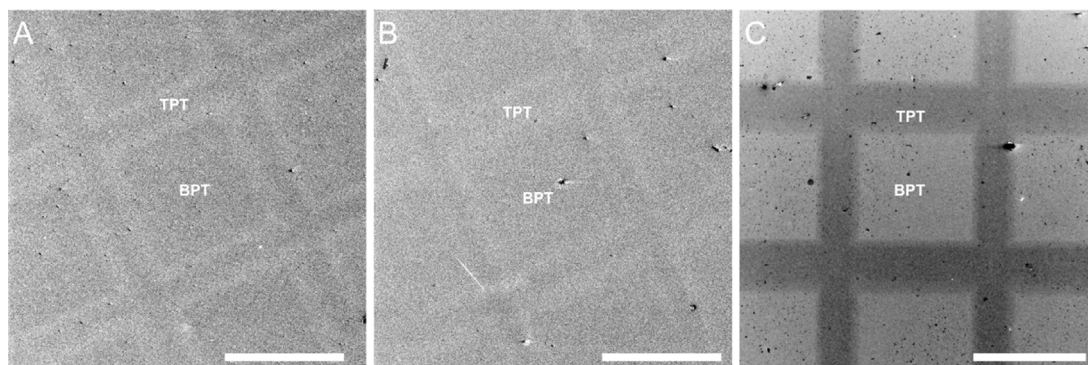
Fig. 3. Analysis of patterned aromatic SAMs by HIM and SEM. Secondary electron (SE) HIM images of a patterned SAM before (A) and after (B) crosslinking by electron irradiation. Apart from a small loss in contrast, the patterns are preserved. (C) SE SEM image of the sample after crosslinking. Scale bars are 100 μm.
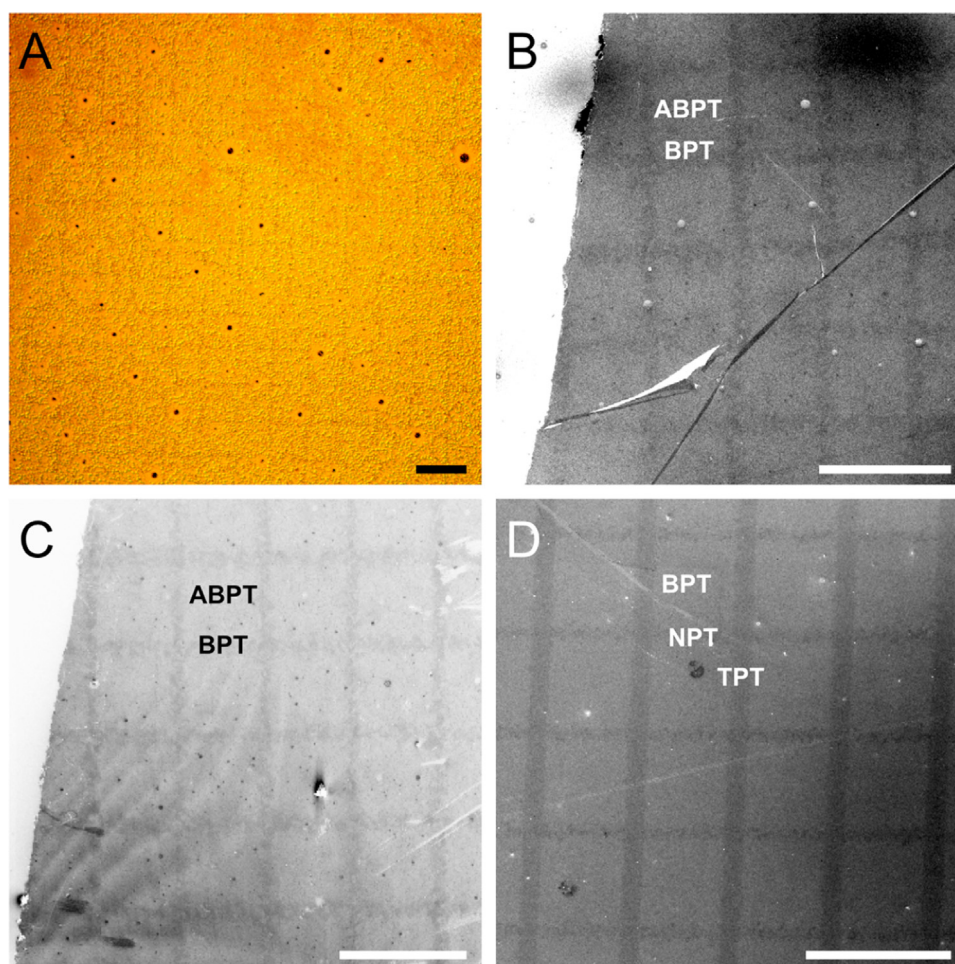

Fig. 4. Structural analysis of patterned CNMs transferred to different substrates. (A) Wetting patterns observed by light microscopy after transfer to a gold substrate. The CNM has been obtained by crosslinking of a NBPT SAM containing lines of BPT. Upon crosslinking, NBPT molecules were converted to amino-terminated molecules (ABPT) [29]. (B) The same sample imaged by HIM and SEM (C). Shown are SE images acquired at the edge of internally patterned CNMs. BPT lines appear darker than the ABPT matrix. (D) SEM image of a patterned CNM, consisting of three aromatic precursor molecules, after transfer to a silicon substrate. Scale bars are 200 μm.

local variation of physical and chemical properties. Future work should address the analysis of mechanical properties of patterned CNM. This could be accomplished by methods, which enable local determination of mechanical properties, such as atomic force microscopy. Combining DLP of SAMs on a solid substrate with subsequent crosslinking resembles a universal scheme for the rapid fabrication of chemically patterned 2D materials with patterns from the biologically relevant micrometer up to the centimeter scale thus widening the spectrum of available nanomembranes [36] with technologically interesting properties.

References

[1] K. Jacobson, O.G. Mouritsen, R.G. Anderson, Lipid rafts: at a crossroad between cell biology and physics, Nat. Cell. Biol. 9 (2007) 7–14.

[2] J.C. Love, L.A. Estroff, J.K. Kriebel, R.G. Nuzzo, G.M. Whitesides, Self-assembled monolayers of thiolates on metals as a form of nanotechnology, Chem. Rev. 105 (2005) 1103–1169.

[3] F. Schreiber, Structure and growth of self-assembling monolayers, Prog. Surf. Sci. 65 (2000) 151–256.

[4] J.Y. Huang, D.A. Dahlgren, J.C. Hemminger, Photopatterning of Self-Assembled Alkanethiolate Monolayers on Gold − a Simple Monolayer Photoresist Utilizing Aqueous Chemistry, Langmuir 10 (1994) 626–628.

[5] M.E. Anderson, M. Mihok, H. Tanaka, L.P. Tan, M.W. Horn, G.S. McCarty, P.S. Weiss, Hybrid approaches to nanolithography: photolithographic structures with precise controllable nanometer-scale spacings created by molecular rulers, Adv. Mater. 18 (2006) 1020–1022.

[6] A. Kumar, G.M. Whitesides, Features of gold having micrometer to centimeter dimensions can be formed through a combination of stamping with an elastomeric stamp and an alkanethiol ink followed by chemical etching, Appl. Phys. Lett. 63 (1993) 2002–2004.

[7] R.D. Piner, J. Zhu, F. Xu, S.H. Hong, C.A. Mirkin, Dip-pen nanolithography, Science 283 (1999) 661–663.

[8] M.J. Lercel, G.F. Redinbo, F.D. Pardo, M. Rooks, R.C. Tiberio, P. Simpson, H.G. Craighead, C.W. Sheen, A.N. Parikh, D.L. Allara, Electron-beam lithography with monolayers of alkylthiols and alkylsiloxanes, J. Vac. Sci. Technol. B 12 (1994) 3663–3667.

[9] A. Golzhauser, W. Eck, W. Geyer, V. Stadler, T. Weimann, P. Hinze, M. Grunze, Chemical nanolithography with electron beams, Adv. Mater. 13 (2001) 803–806.

[10] M.R. Shadnam, S.E. Kirkwood, R. Fedosejevs, A. Amirfazli, Direct patterning of self-assembled monolayers on gold using a laser beam, Langmuir 20 (2004) 2667–2676.

[11] D. Rhinow, N.A. Hampp, Forming microstructured alkanethiol self-assembled monolayers on gold by laser ablation, IEEE Trans. Nanobiosci. 5 (2006) 188–192.

[12] T. Balgar, S. Franzka, E. Hasselbrink, N. Hartmann, Laser-assisted fabrication of submicron-structured hydrophilic/hydrophobic templates for the directed self-assembly of alkylsiloxane monolayers into confined domains, Appl. Phys. A 82 (2006) 15–18.

[13] D. Rhinow, N.A. Hampp, Solid-supported multicomponent patterned monolayers, Adv. Mater. 19 (2007) 1967–1972.

[14] L. Iversen, O. Younes-Metzler, K.L. Martinez, D. Stamou, Chemically specific laser-induced patterning of alkanethiol SAMs: characterization by SEM and AFM, Langmuir 25 (2009) 12819–12824.

[15] D. Rhinow, N.A. Hampp, Patterned self-assembled monolayers of alkanethiols on copper nanomembranes by submerged laser ablation, Appl. Phys. A 107 (2012) 755–759.

[16] A. Schroter, S. Franzka, N. Hartmann, Photothermal laser fabrication of micro- and nanostructured chemical templates for directed protein immobilization, Langmuir 30 (2014) 14841–14848.

[17] J.H. Slater, J.S. Miller, S.S. Yu, J.L. West, Fabrication of multifaceted micropatterned surfaces with laser scanning lithography, Adv. Funct. Mater. 21 (2011) 2876–2888.

[18] W. Geyer, V. Stadler, W. Eck, M. Zharnikov, A. Gölzhäuser, M. Grunze, Electron-induced crosslinking of aromatic self-assembled monolayers: negative resists for nanolithography, Appl. Phys. Lett. 75 (1999) 2401–2403.

[19] W. Eck, A. Küller, M. Grunze, B. Völkel, A. Gölzhäuser, Freestanding nanosheets from crosslinked biphenyl self-assembled monolayers, Adv. Mater. 17 (2005) 2583–2587.

[20] A. Turchanin, A. Beyer, C.T. Nottbohm, X.H. Zhang, R. Stosch, A. Sologubenko, J. Mayer, P. Hinze, T. Weimann, A. Golzhauser, One nanometer thin carbon nanosheets with tunable conductivity and stiffness, Adv. Mater. 21 (2009) 1233–1237.

[21] A. Turchanin, A. Golzhauser, Carbon nanomembranes from self-assembled monolayers: functional surfaces without bulk, Prog. Surf. Sci. 87 (2012) 108–162.

[22] P. Angelova, H. Vieker, N.E. Weber, D. Matei, O. Reimer, I. Meier, S. Kurasch, J. Biskupek, D. Lorbach, K. Wunderlich, L. Chen, A. Terfort, M. Klapper, K. Mullen, U. Kaiser, A. Golzhauser, A. Turchanin, A universal scheme to convert aromatic molecular monolayers into functional carbon nanomembranes, ACS Nano 7 (2013) 6489–6497.

[23] D. Rhinow, M. Buenfeld, N.E. Weber, A. Beyer, A. Golzhauser, W. Kuhlbrandt, N. Hampp, A. Turchanin, Energy-filtered transmission electron microscopy of biological samples on highly transparent carbon nanomembranes, Ultramicroscopy 111 (2011) 342–349.

[24] D. Rhinow, J. Vonck, M. Schranz, A. Beyer, A. Golzhauser, N. Hampp, Ultrathin conductive carbon nanomembranes as support films for structural analysis of biological specimens, Phys. Chem. Chem. Phys. 12 (2010) 4345–4350.

[25] I. Amin, M. Steenackers, N. Zhang, R. Schubel, A. Beyer, A. Golzhauser, R. Jordan, Patterned polymer carpets, Small 7 (2011) 683–687.

[26] A. Turchanin, A. Tinazli, M. El-Desawy, H. Grossann, M. Schnietz, H.H. Solak, R. Tampe, A. Golzhauser, Molecular self-assembly, chemical lithography, and biochemical tweezers: a path for the fabrication of functional nanometer-scale protein arrays, Adv. Mater. 20 (2008) 471–477.

[27] A. Beyer, A. Godt, I. Amin, C.T. Nottbohm, C. Schmidt, J. Zhao, A. Golzhauser, Fully cross-linked and chemically patterned self-assembled monolayers, Phys. Chem. Chem. Phys. 10 (2008) 7233–7238.

[28] A. Schroter, S. Franzka, J. Koch, B.N. Chichkov, A. Ostendorf, N. Hartmann, Femtosecond-laser processing of nitrobiphenylthiol self-assembled monolayers, Appl. Surf. Sci. 278 (2013) 43–46.

[29] W. Eck, V. Stadler, W. Geyer, M. Zharnikov, A. Golzhauser, M. Grunze, Generation of surface amino groups on aromatic self-assembled monolayers by low energy electron beams − A first step towards chemical lithography, Adv. Mater. 12 (2000) 805–808.

[30] G.P. Lopez, H.A. Biebuyck, G.M. Whitesides, Scanning electron-Microscopy can form images of patterns in self-assembled monolayers, Langmuir 9 (1993) 1513–1516.

[31] A.G. Bittermann, S. Jacobi, L.F. Chi, H. Fuchs, R. Reichelt, Contrast studies on organic monolayers of different molecular packing in FESEM and their correlation with SFM data, Langmuir 17 (2001) 1872–1877.

[32] N.H. Mack, R. Dong, R.G. Nuzzo, Quantitative imaging of protein adsorption on patterned organic thin-film arrays using secondary electron emission, J. Am. Chem. Soc. 128 (2006) 7871–7881.

[33] C. Srinivasan, T.J. Mullen, J.N. Hohman, M.E. Anderson, A.A. Dameron, A.M. Andrews, E.C. Dickey, M.W. Horn, P.S. Weiss, Scanning electron microscopy of nanoscale chemical patterns, ACS Nano 1 (2007) 191–201.

[34] G. Hlawacek, V. Veligura, S. Lorbek, T.F. Mocking, A. George, R. van Gastel, H.J.W. Zandvliet, B. Poelsema, Imaging ultra thin layers with helium ion microscopy: utilizing the channeling contrast mechanism, Beilstein J. Nanotechnol. 3 (2012) 507–512.

[35] A. George, M. Knez, G. Hlawacek, D. Hagedoorn, H.H.J. Verputten, R. van Gastel, J.E. ten Elshof, Nanoscale patterning of organosilane molecular thin films from the gas phase and its applications: fabrication of multifunctional surfaces and large area molecular templates for site-selective material deposition, Langmuir 28 (2012) 3045–3052.

[36] J.A. Rogers, M.G. Lagally, R.G. Nuzzo, Synthesis, assembly and applications of semiconductor nanomembranes, Nature 477 (2011) 45–53.